Asian Journal of Pharmaceutical Sciences 19 (2024) 100908

Available online at www.sciencedirect.com

ScienceDirect

journal homepage: www.elsevier.com/locate/AJPS

Research Article

Fine-tuning the activation behaviors of ternary modular cabazitaxel prodrugs for efficient and on-target oral anti-cancer therapy

Mingyang Zhang[a], *Yifan Miao*[a], *Can Zhao*[a], *Tong Liu*[d], *Xiyan Wang*[a], *Zixuan Wang*[a], *Wenxin Zhong*[a], *Zhonggui He*[a,c], *Chutong Tian*[a,b,c,*], *Jin Sun*[a,c,*]

[a] *Department of Pharmaceutics, Wuya College of Innovation, Shenyang Pharmaceutical University, Shenyang 110016, China*
[b] *Key Laboratory of Advanced Drug Delivery Systems of Zhejiang Province, Hangzhou 310058, China*
[c] *Joint International Research Laboratory of Intelligent Drug Delivery Systems, Ministry of Education, Shenyang 110016, China*
[d] *Liaoning Provincial Institute of Drug Inspection and Testing, Shenyang 110036, China*

ARTICLE INFO

Article history:
Received 6 December 2023
Revised 27 January 2024
Accepted 25 February 2024
Available online 30 March 2024

Keywords:
Steric disulfide bond
Triglyceride-like prodrugs
Cabazitaxel
Lymphatic transport
Oral chemotherapy

ABSTRACT

The disulfide bond plays a crucial role in the design of anti-tumor prodrugs due to its exceptional tumor-specific redox responsiveness. However, premature breaking of disulfide bonds is triggered by small amounts of reducing substances (*e.g.*, ascorbic acid, glutathione, uric acid and tea polyphenols) in the systemic circulation. This may lead to toxicity, particularly in oral prodrugs that require more frequent and high-dose treatments. Fine-tuning the activation kinetics of these prodrugs is a promising prospect for more efficient on-target cancer therapies. In this study, disulfide, steric disulfide, and ester bonds were used to bridge cabazitaxel (CTX) to an intestinal lymph vessel-directed triglyceride (TG) module. Then, synthetic prodrugs were efficiently incorporated into self-nanoemulsifying drug delivery system (corn oil and Maisine CC were used as the oil phase and Cremophor EL as the surfactant). All three prodrugs had excellent gastric stability and intestinal permeability. The oral bioavailability of the disulfide bond-based prodrugs (CTX-(C)S-(C)S-TG and CTX-S-S-TG) was 11.5- and 19.1-fold higher than that of the CTX solution, respectively, demonstrating good oral delivery efficiency. However, the excessive reduction sensitivity of the disulfide bond resulted in lower plasma stability and safety of CTX-S-S-TG than that of CTX-(C)S-(C)S-TG. Moreover, introducing steric hindrance into disulfide bonds could also modulate drug release and cytotoxicity, significantly improving the anti-tumor activity even compared to that of intravenous CTX solution at half dosage while minimizing off-target adverse effects. Our findings provide insights into the design and fine-tuning of different disulfide bond-based linkers, which may help identify oral prodrugs with more potent therapeutic efficacy and safety for cancer therapy.

* Correspondence authors.
E-mail addresses: tianct_spu@126.com (C. Tian), sunjin@syphu.edu.cn (J. Sun).
Peer review under responsibility of Shenyang Pharmaceutical University.

https://doi.org/10.1016/j.ajps.2024.100908

1. Introduction

Oral chemotherapy has always been a hot topic in clinical research owing to its advantages of convenient and flexible administration, good patient compliance, and high safety [1]. Taxane-based therapy had become the main method to treat various solid tumor types. However, the anti-tumor activity of paclitaxel and docetaxel was limited by multidrug resistance proteins (*e.g.*, P-glycoprotein (P-gp)). By contrast, cabazitaxel (CTX) stood out due to its high cytotoxicity and low affinity for P-gp. As the first chemotherapeutic drug to prolong the survival of patients with castration-resistant prostate cancer that is resistant to docetaxel, CTX is widely used clinically [2,3]. However, drug delivery through the oral route is limited, which could be attributed to the non-drug-like properties of chemotherapy drugs, such as poor water solubility, low membrane permeability, and a high hepatic first-pass effect [4,5]. Besides, gastrointestinal toxicity also impedes its oral delivery [6,7]. Intestinal lymphatic transport could bypass the hepatic first-pass effect and improve the oral bioavailability of the active drug [8]. In recent years, nanotechnology, such as nanoemulsions, lipid nanoparticles, and self-microemulsions, has been applied to improve the lymphatic transport of drugs [9–12]. However, lymphatic transport efficiency and gastrointestinal tract safety are affected by the premature leakage of chemotherapy drugs. Therefore, prodrug strategies are typically employed to improve the physical and chemical properties of the active drugs and reduce off-target toxicity [13–15]. Commonly, these prodrugs consist of three modules: an active drug (CTX), a recognizing unit towards the intestinal lymphatic system, and a responsive linker specifically cleavable at the tumor sites.

Lipids such as fatty acids, glycerides, phospholipids, and steroids are usually used to design lipid-like prodrugs owing to their lymphatic-targeting properties [16–19]. Lipidated prodrugs are usually formed by covalently linking the drug to a fatty acid chain [20–22]. Although this strategy improves the lipophilicity of the active drug, its development has been hindered by its limited lymphatic-targeting ability and potential gastrointestinal toxicity. Triglycerides (TGs) are the main components of animal and vegetable fats and play an important role in human life [23]. Lipase exists widely in the human body and is highly expressed in tumor sites [24]. After entering the human body, TG is hydrolyzed into 2-monoglyceride (2-MG) and free fatty acids by pancreatic lipases [25]. Subsequently, 2-MG passes through the unstirred water layer (UWL) into the small intestinal epithelial cells as mixed micelles [26]. 2-MG was re-esterified with exogenous or endogenous long-chain fatty acids and reassembled with phospholipids, cholesterol and apolipoproteins to form lipoproteins (LPs) [27]. LPs are then transported into the systemic circulation via the lymphatic system, bypassing the first-pass effect [28]. Inspired by this physiological pathway, TG-like prodrugs of active drugs with different structures and utilities (including testosterone, mycophenolic acid, paclitaxel and SN38) have been developed, and their ability to promote lymphatic transport has been proven. These previous studies confirmed that TGs could serve as lymph vessel-directed module to improve oral drug delivery efficiency [29–32].

For oral chemotherapy, tumor-triggered bioactivation of prodrugs is indispensable for boosting on-site anti-tumor effects. Tumor cells are heterogeneous in pH, enzymes, and redox environments compared to normal cells [33,34]. Based on the above condition, many sensitive bonds (*e.g.*, pH- and enzyme-sensitive bonds) have been developed for the responsive release of drugs. However, pH-sensitive bonds had a narrow sensitive range, and enzyme-sensitive bonds were difficult to release the drug completely, which greatly limited the drug delivery *in vivo* treatment. Due to their outstanding redox sensitivity [35–37], disulfide bonds are widely used in the design of prodrugs. In our previous study, disulfide bond-bridged TG-like docetaxel prodrugs were designed, which showed promising oral anti-tumor efficacy [38]. However, we also found that much of the active drug was released into blood circulation. This relative instability leads to a potential risk of off-target toxicity when the active drug has high cytotoxic activities [39–41]. Hence, the rational design of a response module with improved blood stability and rapid on-demand drug release from tumor cells remains a great challenge. Inspired by the design of antibody-drug conjugates (ADCs), the stability of disulfide bonds could be adjusted by introducing steric hindrance [42,43]. Brenda et al. demonstrated that conjugates with methyl steric hindrance on both sides of the disulfide bond are more stable than those without steric hindrance [44]. Additionally, the *in vitro* reduction stability of the conjugate was enhanced by an increase in the steric hindrance around the disulfide bonds. ADC drugs are complexes formed by connecting antibodies and small molecular drugs through a specific linker, which are usually administered by intravenous injection. However, there are many differences between single small molecule drugs and ADC drugs in terms of physicochemical properties and *in vivo* fate. Moreover, oral chemotherapy needs to overcome the harsh gastrointestinal environment and premature drug release in blood circulation. At present, the role of steric hindrance modification in oral chemotherapy has not been mentioned. Therefore, we speculate that masking disulfide bonds with α- alkyl substitutions could influence its chemical stability and further improve prodrug safety. To the best of our knowledge, the application of steric disulfide bonds as response modules in the field of oral prodrug delivery has not yet been reported, and the differences in the oral anti-tumor effects and safety of fine-tuning the activation kinetics of these prodrugs remain unknown.

In light of the above considerations, a series of TG-like CTX prodrugs were designed and synthesized, in which the disulfide, steric disulfide, and ester bonds were utilized as response modules to bridge CTX to the intestinal lymph vessel-directed triglyceride module. TG-like CTX prodrugs were efficiently encapsulated into SNEDDS (oil phase: surfactant = 70:30) and could be spontaneously emulsified to form nanoemulsions *in vivo*. The impacts of different bonds on the chemical stability and *in vivo* fate of prodrugs were discussed in detail. The GI stability and the differences in reduction responsivity between disulfide bonds, steric disulfide bonds, and ester bonds were examined, while their influence on cytotoxicity was elucidated. As shown in Fig. 1, TG-like prodrugs can enter blood circulation smoothly through lymphatic transport. Compared to disulfide bonds,

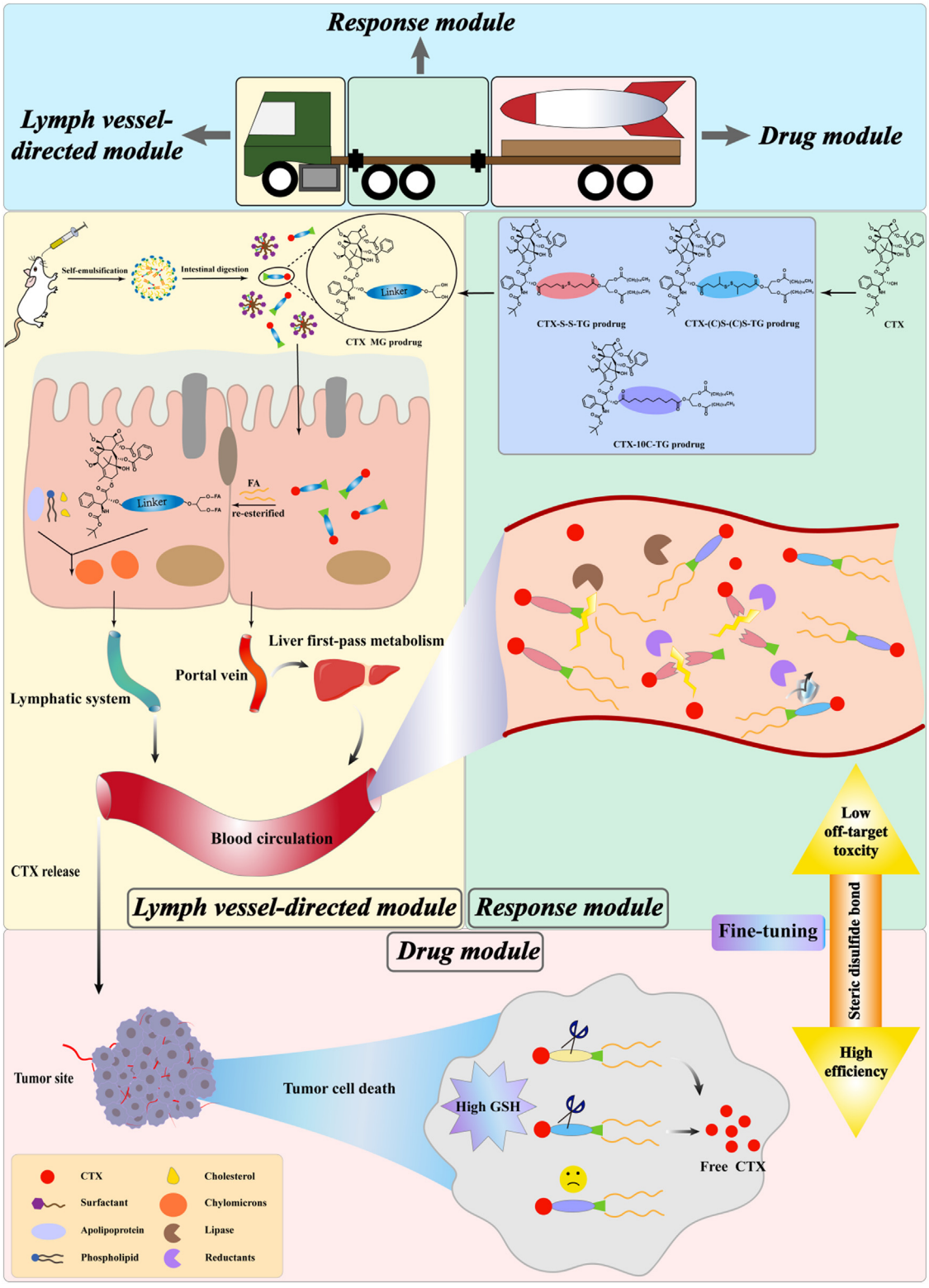

Fig. 1 – *In vivo* fate diagram of TG-like CTX prodrugs after oral administration.

steric disulfide bonds have more desirable chemical inertia, which greatly improves the plasma stability and systemic safety of the prodrug. Steric disulfide bond-bridged TG-like prodrugs also exhibit acceptable reduction-responsive drug release, effectively killing tumor cells. CTX-(C)S-(C)S-TG prodrugs with steric disulfide bond showed modest reduction sensitivity and decreased systemic toxicity, integrating anti-tumor efficacy with enhanced safety. Thus, fine-tuning the activation behaviors can decrease the reduction sensitivity of disulfide bonds to avoid premature release of active drugs in blood circulation, which provides novel insights for developing safer and more effective oral drug delivery systems.

2. Materials and methods

2.1. Materials

CTX was purchased from Nanjing Dilger Medical Technology Co., Ltd. Corn oil was obtained from Shandong Ruisheng Pharmaceutical Excipient Co., Ltd (Shandong, China). Maisine CC was bought from Gattefossé (Shanghai) Trade Co., Ltd (Shanghai, China). 4,4′-dithiodibutyric acid, 1-ethyl-3-(3-dimethylaminopropyl) carbodiimide hydrochloride (EDCI), 4-dimethylaminopyridine (DMAP), dithiothreitol (DTT) and verapamil hydrochloride were purchased from Shanghai Aladdin Biochemical Technology Co., Ltd. (Shanghai, China). 4,4′′-disulfanediyldipentanoic acid was obtained from RuixiBiotech Co. Ltd. (Xian, China). 3-(4,5-dimethylthiazol-2-yl)-2,5-diphenyl tetrazolium bromide (MTT) and tris (2-carboxyethyl) phosphate (TCEP) were purchased from Dalian Meilun Biotechnology Co., Ltd. (Dalian, China). Lipoprotein lipase was bought from Novocata Biotechnology Co., Ltd. (Hangzhou, China). All other solvents and reagents used were of analytical quality.

2.2. Synthesis of the triglyceride-like CTX prodrugs

Three prodrugs of CTX: CTX-S-S-TG, CTX-(C)S-(C)S-TG and CTX-10C-TG, were synthesized and their synthetic routes were shown in Scheme S1. The chemical structures of the triglyceride-like CTX prodrugs were confirmed by high-resolution mass spectra (HPLC Waters ACQUITY Arc, ESI MS), ^{1}H NMR and ^{13}C NMR (Bruker AVIII-400 M NMR). Specific steps are represented in the supplementary materials.

2.3. Preparation of triglyceride-like prodrugs lipid-based formulations

First, 350 mg corn oil, 350 mg Maisine CC and 300 mg Cremophor EL were mixed and sonicated to obtain a uniform blank preparation. Herein, corn oil and Maisine CC were used as the oil phase and Cremophor EL as the surfactant. Then, 20 mg prodrugs or 10 mg CTX were dissolved in the blank preparation.

In order to explore the equilibrium solubility of lipid-based formulations, 100 mg CTX-S-S-TG, CTX-(C)S-(C)S-TG, CTX-10C-TG and CTX were added to the blank preparation, respectively. The medicated lipid-based preparations were placed in the thermostatic oscillator at 37 °C for 72 h. Subsequently, the undissolved drugs in the lipid-based formulations were separated after centrifuging at 13,000 rpm for 30 min. Acetonitrile (1 ml) was added to the 20 μl of various medicated preparations, and the concentration of the prodrugs or CTX was analyzed by high-performance liquid chromatography (HPLC).

2.4. Characterization of self-nanoemulsifying drug delivery system

Self-nanoemulsifying drug delivery system (SNEDDS) is a solid or liquid preparation containing drugs, oil phase, surfactant and co-surfactant, which spontaneously emulsifies to form oil-in-water (O/W) emulsion in the environment of gastrointestinal peristalsis. SNEDDS has the advantages of simple preparation process, high drug load and easy scale-up, which is suitable for delivery of oral lipid prodrugs. In order to investigate the dispersion of SNEDDS in stomach, 100 μl prodrugs or CTX SNEDDS were dripped into 900 μl distilled water under stirring. The particle size and polydispersity index (PDI) of the emulsion particles in SNEDDS were estimated by the Zetasizer particle size analyzer (Malvern, UK). Moreover, transmission electron microscopy (TEM) was applied to observe the morphology of the emulsion particles.

2.5. Gastrointestinal behavior studies

2.5.1. Stability in simulated gastric fluid

As mentioned in the previous literature, simulated gastric fluid (SGF) was prepared to be utilized as the release medium [45]. Then, the physical stability of the CTX prodrug SNEDDS was investigated. SNEDDS (1 ml) was added to SGF (9 ml) and incubated with gentle shaking at 37 °C. At different intervals (0, 30, 60, 120, 180 and 240 min), 100 μl mixed solution was extracted and added to 900 μl distilled water to measure the particle size. Afterward, the physical stability of the CTX prodrug SNEDDS was investigated. 100 μl mixed solution was obtained and taken out according to the previous method and added to 300 μl acetonitrile to analyze the concentration of the CTX prodrugs by HPLC. Experiments were repeated for three times.

2.5.2. Drug release in SGF

The *in vitro* drug release of CTX, CTX-S-S-TG, CTX-(C)S-(C)S-TG, CTX-10C-TG SNEDDS and CTX solution in SGF were investigated by the dialysis method. SGF was used as release media, containing 30% ethanol (v/v) to achieve sink conditions [46,47]. The pH value of the SGF was 1.2. The dialysis bags (10 kD, 12 mm) were filled with 100 μl prodrugs, CTX SNEDDS and CTX solution (0.2 mg equivalent to CTX), respectively. Then, they were soaked in 30 ml release media. The 100 μl mixture solution was collected at predetermined intervals (0, 0.25, 0.5, 1, 2, 4 and 6 h) after incubating with gentle shaking at 37 °C. Then, the concentration of prodrugs and CTX were analyzed by HPLC. Experiments were repeated three times.

2.5.3. Simulated intestinal digestion

According to the previous literature, simulated intestinal fluid (SIF) was prepared [48]. In order to simulate digestion in the intestinal tract, 200 μl prodrugs or CTX SNEDDS were added to 3.8 ml simulated digestive fluid and incubated with gentle shaking at 37 °C. Then, 50 μl incubation solution was extracted at different times (0, 5, 15, 30, 60 and 120 min) and added to 150 μl acetonitrile. Subsequently, the concentrations of TG prodrugs and MG derivatives of CTX (2-MG prodrugs) were determined by HPLC. Bioaccessibility refers to the percentage of the drug that is ingested and utilized by the human body after entering the gastrointestinal tract (GIT). To analyze the bioaccessibility of prodrugs or CTX SNEDDS, the solubility of prodrugs and CTX in the intermediate aqueous phase was measured. 50 μl incubation solution was obtained and extracted according to the aforementioned method. Subsequently, the samples were centrifuged at 13,000 rpm

for 10 min at 4 °C. The samples were separated into the oil phase at the top, the aqueous phase in the middle and the pellet phase at the bottom. Then, 20 μl aqueous phase was mixed with 180 μl acetonitrile to measure the concentrations of the 2-MG prodrugs, TG prodrugs and CTX. Experiments were repeated three times.

2.6. Cell culture

Mouse prostate cancer cell line (RM-1 cells), human breast cancer cell line (MCF-7), mouse embryonic fibroblast cell line (3T3 cells) and human colon cancer cell line (Caco-2) were obtained from the cell bank of Type Culture Collection of Chinese Academy of Sciences (Beijing, China). RM-1 cells were cultured in RPMI 1640 medium with 10% fetal bovine serum (FBS), 1% penicillin (10 KU/ml) and 1% streptomycin (10 mg/ml), while 3T3 cells were cultured in DMEM/F-12 medium containing the same serum and antibiotics. MCF-7 and Caco-2 cells were cultured in DMEM with 10% and 20% FBS, respectively. All cells were stored in a humidified cell incubator with 5% CO_2 and 37 °C.

2.7. Caco-2 cellular uptake study

Caco-2 cells are similar to differentiated small intestinal epithelial cells in structure and function, which can be used to simulate intestinal transport *in vivo* and explore the intestinal absorption mechanism of drugs. Caco-2 cells were inoculated in 12-well plates (5×10^4 cells per well) for 24 h to investigate the cell uptake of prodrugs and CTX. Subsequently, the nutrient-free medium was replaced with fresh medium containing CTX, CTX-S-S-TG, CTX-(C)S-(C)S-TG, CTX-10C-TG SNEDDS and CTX solution (equivalent CTX concentration of 5 μg/ml) and cells were incubated for 1 or 3 h at 37 °C. At the end of incubation, Caco-2 cells were washed with ice-cold phosphate buffer solution (PBS) three times to terminate cellular uptake. Cells were suspended in 200 μl distilled water and disrupted by ultrasound (100 W). Before centrifugation, the concentration of CTX was evaluated by a multifunctional enzyme reader. The lysing agent was added to the cell suspension and the mixture was centrifuged at 13,000 rpm for 10 min. The concentrations of CTX were measured by HPLC. Verapamil was used as the P-glycoprotein (P-gp) inhibitor to investigate the effect of P-gp on intestinal penetration of CTX prodrugs. Caco-2 cells were cultured in the medium with CTX, CTX-S-S-TG, CTX-(C)S-(C)S-TG, CTX-10C-TG SNEDDS and CTX solution (equivalent CTX concentration of 5 μg/ml) and verapamil (50 μg/ml) for 1 or 3 h at 37 °C. The handling method was the same as above.

2.8. In vitro reduction release of prodrugs

The redox-responsivity of disulfide bonds could specifically respond to the overproduced glutathione (GSH) in tumor cells. As a result, disulfide bonds-bridged CTX TG-like prodrugs could specifically release the active drug in tumor sites. In order to explore the reduction-sensitivity of CTX prodrugs, dithiothreitol (DTT, a common substitute of GSH) was used to simulate the reduction environment of drug release *in vitro*. PBS (pH 7.4, containing 30% ethanol) with or without DTT was utilized as the release media to investigate the reduction release of CTX prodrugs. The concentration of DTT was selected at 10 mM and 50 mM in reduction-sensitive release medium. Subsequently, 200 μl prodrug SNEDDS (CTX-S-S-TG, CTX-(C)S-(C)S-TG and CTX-10C-TG) were encapsulated into the dialysis bags and incubated in 20 ml release media with or without DTT at 37 °C. At predetermined intervals (0, 1, 2, 4, 6, 8, 12, 24 and 48 h), a 200 μl incubated sample was taken out, and an equal volume of fresh release media was supplemented to maintain the original volume. The concentration of CTX released from prodrugs was determined by HPLC. Experiments were repeated three times.

2.9. Stability of the prodrugs in rat plasma

The blank rat plasma was acquired from Sprague–Dawley (SD) rats to analyze the stability of the linkers in the systemic circulation. Then, 100 μl prodrug SNEDDS were added to 400 μl rat plasma supplemented with lipase (1,000 IU/ml) activity and incubated at 37 °C with gentle shaking. Thereafter, 20 μl incubation solutions were taken at predetermined times (0, 0.5, 1, 2, 4, 8 and 12 h) and added to 180 μl acetonitrile to determine the concentration of 2-MG prodrugs and free CTX by HPLC. In order to simulate the tumor environment, TG prodrugs were incubated with rat plasma supplemented with lipase (1,000 IU/ml) and high concentration of DTT (50 mM). Similarly, the concentration of 2-MG prodrugs and free CTX were analyzed according to the aforementioned method. Experiments were repeated three times.

2.10. In vitro cytotoxicity assay

The cytotoxicity of CTX-S-S-TG, CTX-(C)S-(C)S-TG, CTX-10C-TG SNEDDS and CTX solution against RM-1, MCF-7 and 3T3 cells were investigated by MTT assays. In brief, cells were seeded into 96-well plates (3,000 cells per well) and cultured for 24 h. The nutrient-free medium was replaced with different concentrations of multifarious prodrugs and CTX solution. Cells were cultured for 48 h or 72 h. Wells containing only substrate and wells inoculated with untreated cells were utilized as blank and control groups, respectively ($n = 3$ for each group). The absorbance of each group was detected by the microplate reader (SYNERGY, BioTek Instruments, Inc, USA). The half-maximal inhibitory concentration (IC_{50}) values were calculated by GraphPad Prism. Then, the SI was calculated as the ratio of the IC_{50} of the 3T3 cells divided by that of the tumor cell lines. Caco-2 was used as experimental cells to investigate the enterotoxicity of CTX-S-S-TG, CTX-(C)S-(C)S-TG, CTX-10C-TG SNEDDS, CTX SNEDDS and CTX solution by MTT assays. Caco-2 cells were seeded into 96-well plates (5,000 cells per well) and cultured for 48 h. The nutrient-free medium was replaced with different concentrations of multifarious prodrugs, CTX SNEDDS and CTX solution. Cells were cultured for 4 h, 8 h or 12 h. The next steps were the same as above.

2.11. Animal studies

SD rats (180-220 g) and C57BL/6 mice (18-22 g) were provided by the Animal Center of Shenyang Pharmaceutical University.

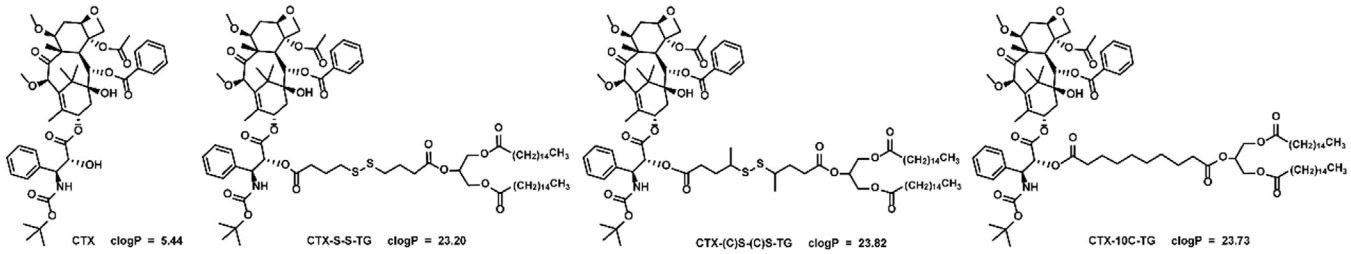

Fig. 2 – Chemical structures of CTX and TG-like CTX prodrugs.

All the animal experiments were in accordance with the guidelines for the Care and Use of Laboratory Animals provided by the Institutional Animal Ethical Care Committee of Shenyang Pharmaceutical University.

2.12. *In vivo oral pharmacokinetic study*

Male SD rats (190-220 g) were selected as model animals to estimate the oral absorption of CTX triglyceride-like prodrugs. The rats were divided into 5 groups randomly and fasted for 12 h ($n = 3$). Each group was orally administrated with CTX solution (15 mg/kg), CTX emulsion (15 mg/kg), CTX-S-S-TG prodrug emulsion, CTX-(C)S-(C)S-TG prodrug emulsion and CTX-10C-TG prodrug emulsion (15 mg/kg equivalent to CTX). Then, 0.5 ml blood samples of each group were placed into heparin sodium pre-coated EP tubes at scheduled intervals (0.08, 0.25, 0.5, 1, 1.5, 2, 4, 6, 8, 12, 24 h). In order to calculate absolute bioavailability, three SD rats were intravenously administrated with CTX solution (15 mg/kg). Colchicine was selected as the lymphatic transport inhibitor to investigate the absorption pathway of prodrugs. Rats were intraperitoneally injected with colchicine (5 mg/kg) 1 h before oral administration of CTX solution and prodrugs emulsion. All of the blood samples were centrifuged immediately at 13,000 rpm for 3 min and the extracted plasma was stored at −80 °C until analysis. The protein precipitation method was used to estimate the concentration of CTX. Tris (2-carboxyethyl) phosphine (TCEP) and lipase were selected to cut the structure of the prodrug to determine the total CTX concentrations of CTX-S-S-TG and CTX-(C)S-(C)S-TG groups. In short, 50 μl lipase (10,000 IU/ml) and 20 μl TCEP (1 mM for CTX-S-S-TG and 4 mM for CTX-(C)S-(C)S-TG) were added in turn to 50 μl plasma samples, then they were mixed for 5 min by vortex mixer to release CTX by splitting the ester bond and disulfide bond of prodrugs. The following processes were the same as the above method for the determination of free CTX. DAS 2.0 software was applied to calculate the pharmacokinetic parameters. The relative bioavailability (F_{rel}) and absolute bioavailability (F_{ab}) were calculated as follows:

$$F_{rel} = AUC_{emulsion} \times Dose_{Sol} / AUC_{Sol} / Dose_{emulsion}$$

$$F_{ab} = AUC_{p.o} \times Dose_{i.v.} / AUC_{i.v.} / Dose_{p.o.}$$

Where, $AUC_{emulsion}$ and $Dose_{emulsion}$ are the corresponding parameters of emulsion product, AUC_{Sol} and $Dose_{Sol}$ are the corresponding parameters of the reference product, $AUC_{p.o.}$ and $Dose_{p.o.}$ are the corresponding parameters of the formulations administrated orally (p.o.), $AUC_{i.v.}$ and $Dose_{i.v.}$ are the corresponding parameters of the intravenous (i.v.) CTX.

2.13. *In vivo anti-tumor effect*

Male C57BL/6 mice inoculated with RM-1 cell line were used as the tumor model (xenograft tumor model) to investigate the *in vivo* anti-tumor effect of TG prodrugs. PBS suspension of RM-1 cells was ectopically inoculated into the back of male C57BL/6 mice to establish the tumor model. When the tumor volume reached 70 mm^3, the mice were orally administered with saline, CTX solution, CTX emulsion and CTX triglyceride-like prodrugs emulsion (CTX-S-S-TG, CTX-(C)S-(C)S-TG and CTX-10C-TG, CTX equivalent concentration 5 mg/kg) or intravenously administered CTX solution at a dose of 5 mg/kg ($n = 5$ each group). Oral administration was performed daily, while CTX solution was intravenously treated every 3 d Tumor volume and body weight were estimated and calculated every day. After the measurement at Day 10, plasma was collected for hepatorenal function analysis and blood routine examination. The mice were sacrificed tenderly. Then, major organs and tissues (heart, liver, spleen, lung, kidney, stomach, duodenum, jejunum, ileum and colon) were collected and fixed in 4% paraformaldehyde solution. The detached tumors were weighed and used for hematoxylin and eosin (H&E) staining together with major organs and tissues. In addition, unvaccinated mice were orally administered with saline, CTX-S-S-TG and CTX-(C)S-(C)S-TG (30 mg/kg) to investigate the safety of reduction-sensitive prodrugs at high doses. The weight of mice was measured every day and plasma was collected on the last day for blood routine examination.

2.14. *Statistical analysis*

GraphPad Prism 8.0 was used to dispose the data as the mean ± SD. Two-group comparisons were analyzed with Student's *t*-test. Statistical significances were considered at *P* values < 0.05, < 0.01, < 0.001, and < 0.0001.

3. Results and discussion

3.1. *Design and synthesis of prodrugs*

CTX-S-S-TG was synthesized by conjugating CTX to a triglyceride skeleton via a reduction-sensitive disulfide bond. To estimate the influence of the response module fine-tuning on the safety and anti-tumor efficacy of the prodrugs,

Table 1 – Characterization of CTX and prodrug-loaded emulsions ($n = 3$).

Formulations	Size (nm)	PDI	Equilibrium solubility (mg/g)
CTX SNEDDS	68.21±1.07	0.36±0.023	12.8 ± 1.27
CTX-S-S-TG SNEDDS	69.03±2.22	0.37±0.010	70.6 ± 4.56
CTX-(C)S-(C)S-TG SNEDDS	68.94±1.45	0.38±0.022	71.1 ± 3.02
CTX-10C-TG SNEDDS	67.18±5.50	0.34±0.039	71.7 ± 6.41

CTX-(C)S-(C)S-TG and CTX-10C-TG were synthesized. Their chemical structures (Fig. 2) were confirmed by mass spectroscopy, ^{1}H NMR and ^{13}C NMR (Figs. S1–S9). The prodrugs showed higher calculated lipophilicity (clogP) values than CTX, indicating that the triglyceride module could improve the lipophilicity of chemotherapeutic drugs.

3.2. *Dispersion and characterization of lipid-based formulations*

Three prodrug-loaded lipid-based formulations were prepared for subsequent experiments. As shown in Table 1, the improved equilibrium solubility of the three prodrugs (>70 mg/g) was guaranteed because of their excellent lipophilicity, which was significantly higher than that of CTX (12.8 mg/g). Self-emulsified nanoemulsions with a blue opalescent appearance were obtained after dispersing the lipid-based formulations in distilled water, with droplet sizes of approximately 70 nm and a PDI of less than 0.4 (Table 1). It proved that SNEDDS had a good gastrointestinal dispersion, which was conducive to subsequent digestion. The TEM images clearly confirmed the successful fabrication of emulsions with a spherical structure (Fig. 3). These results suggest that lipid-based formulations have excellent self-emulsifying capacity, which is conducive to the formation of homogeneous emulsion droplets after oral administration.

3.3. *Gastrointestinal behavior studies*

3.3.1. *Stability and drug release in SGF*

As shown in Fig. 4A and 4B, prodrug SNEDDS showed no significant changes in particle size or content after incubation with SGF. The results demonstrated that the three prodrug SNEDDS had excellent physical and chemical stability with no notable leakage of the parent drug, thereby avoiding potential gastric toxicity. The gastric release profiles of CTX and prodrugs from SNEDDS are shown in Fig. 4C. When incubated with SGF for 2 h, more than 30% and 50% of CTX were released from the CTX SNEDDS and CTX solutions, respectively. In contrast, the amount of the three prodrugs released from SNEDDS was negligible, indicating a stronger binding ability of the prodrugs with lipid excipients in SNEDDS. Consequently, good gastric stability and acceptable drug release could ensure intestinal digestion and absorption of prodrugs.

3.3.2. *Simulated intestinal digestion*

The TG-like CTX prodrug-loaded lipid-based formulations were dispersed in SIF, and the ability of prodrugs with a lymph vessel-directed module to mimic the digestion and absorption of dietary TGs was verified. The 2-MG prodrugs were generated by the hydrolysis of palmitic acid at positions 1 and 3 of the triglyceride structures by lipase. The formation of 2-MG prodrugs was confirmed by high-resolution mass spectrometry (Figs. S10–S12). As shown in Fig. 4D, the TG-like prodrugs were almost completely digested by lipase within 30 min. Notably, the digestion rate of the CTX-(C)S-(C)S-TG prodrug was slightly reduced owing to steric hindrance on both sides of the disulfide bond. Correspondingly, the 2-MG prodrug produced from the CTX-(C)S-(C)S-TG prodrug was more stable in the intestine than that produced from the CTX-S-S-TG prodrug (Fig. 4E). Additionally, the generation rate of the 2-MG prodrugs coincided with the digestion rate of the TG prodrugs, approaching 100% after 30 min

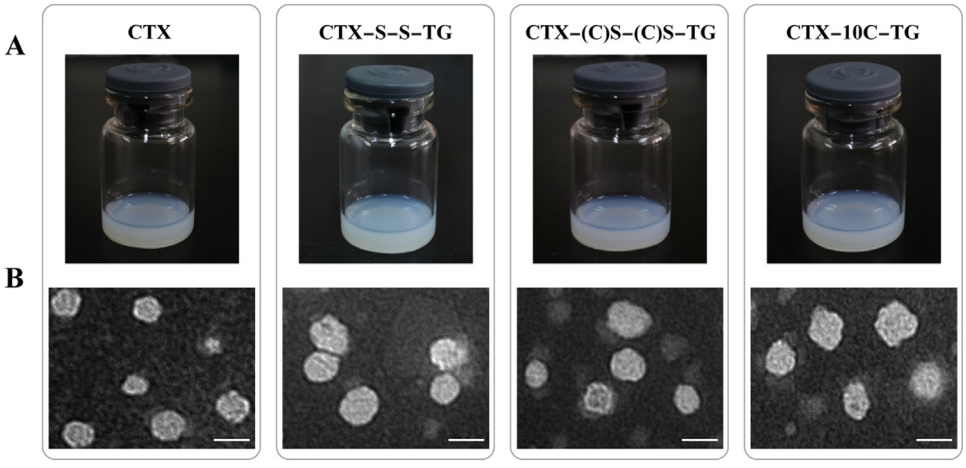

Fig. 3 – (A) Appearances and (B) TEM images of CTX and TG-like prodrugs-loaded emulsions in SGF (Scale bar represents 50 nm).

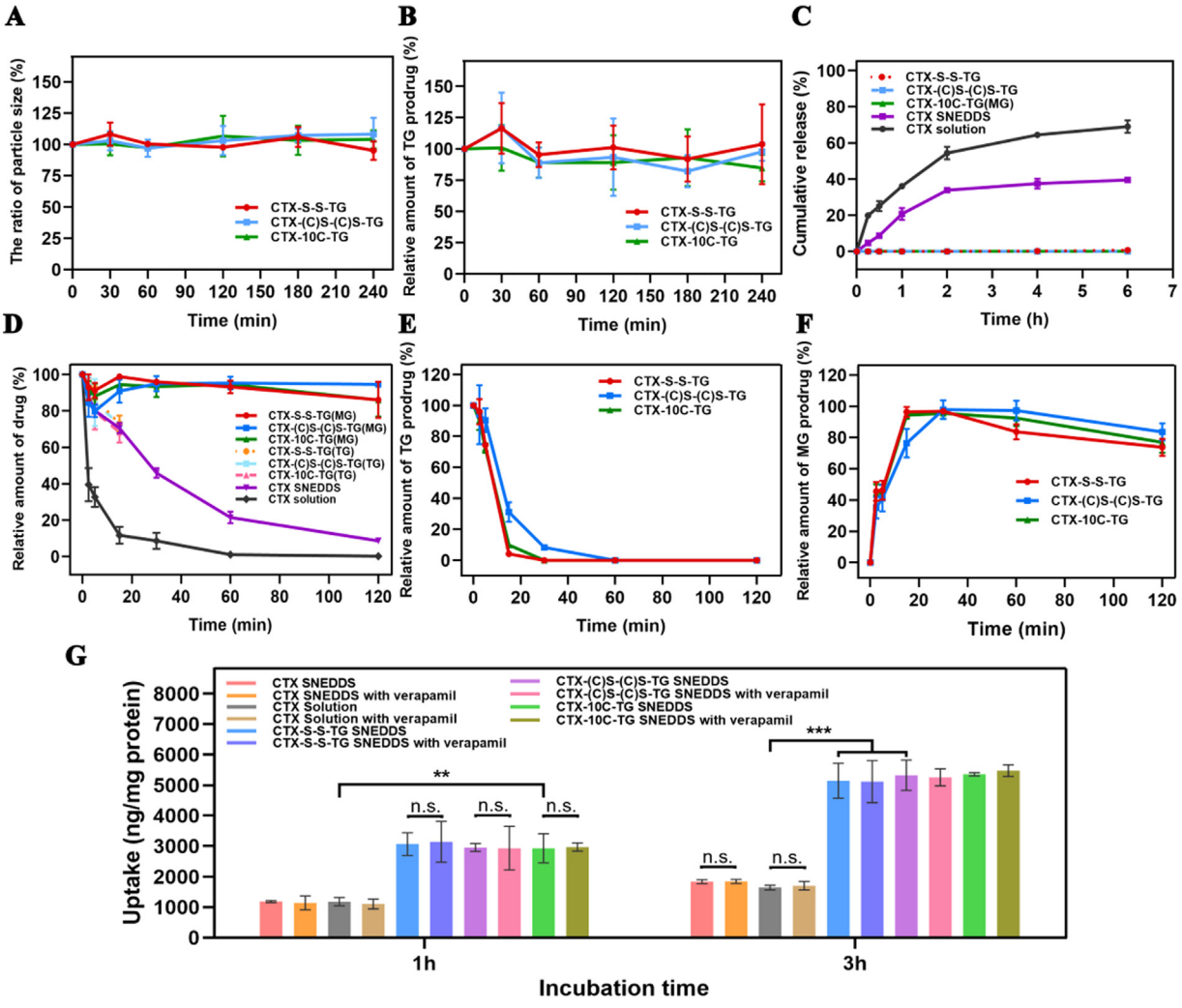

Fig. 4 – Gastrointestinal behavior of TG-like prodrugs. (A) Physical stability of TG-like prodrug SNEDDS in SGF. (B) Chemical stability of TG-like prodrugs in SGF. (C) *In vitro* drug release of CTX TG-like prodrugs and CTX SNEDDS in SGF. (D) The fraction of TG-like prodrugs or MG-like prodrugs partitioning in the mixed micellar phase after 2 h digestion of three prodrugs. (E) Chemical stability of TG-like prodrugs in bile-pancreatic juice. (F) Generation of MG prodrugs after incubation with bile-pancreatic juice. (G) Cellular uptake in Caco-2 cells incubated with CTX solution, CTX SNEDDS, and CTX prodrug SNEDDS with or without verapamil for 1 and 3 h evaluated by HPLC. Data are presented as mean ± SD ($n = 3$); $^{**}P < 0.01$, $^{***}P < 0.001$.

(Fig. 4E). These results showed that the lymph vessel-directed module endowed prodrugs with the ability to simulate the digestion process of natural TGs, which was conducive to the subsequent absorption of prodrugs.

Thereafter, the CTX prodrug content in the intermediate aqueous layer was measured to determine its intestinal absorption. At each digestion point in time, the digestive mixtures were centrifuged at 4 °C into the upper oil phase, the intermediate aqueous phase, and the bottom precipitated phase. The aqueous phase was mainly composed of mixed micelles formed by drugs with bile acids, phospholipids, and other digestive products. As shown in Fig. 4F, almost all the parent drugs of the CTX SNEDDS and CTX solution groups precipitated from the aqueous phase after 1 h of digestion, which might be attributed to the poor affinity of CTX for mixed micelles. In contrast, 86%, 94.6% and 86% of the corresponding 2-MG prodrugs in the three CTX prodrug SNEDDS groups were distributed in the aqueous phase. The digested prodrugs and lipid excipients formed mixed micelles more easily, facilitating prodrug crossing over the UWL to enhance subsequent intestinal absorption. The above results preliminarily showed that TG-like prodrugs with a lymph vessel-directed module can mimic the digestion of dietary TGs.

3.4. *Caco-2 cellular uptake*

Caco-2 cells are structurally and functionally similar to differentiated intestinal epithelial cells, which can be used to mimic *in vivo* intestinal transport and investigate the

intestinal permeability of drugs [49–51]. As shown in Fig. 4G, the cellular uptake of CTX and prodrugs increased with incubation time. Moreover, the uptake of the three prodrug SNEDDS groups by Caco-2 cells was stronger than that of the CTX SNEDDS and CTX solutions. After 3 h of incubation, the intracellular parent drug concentrations in the CTX-S-S-TG and CTX-(C)S-(C)S-TG SNEDDS groups were 3.1- and 3.2-fold higher, respectively, than those in the CTX solution group. The increase in cell uptake indicates that prodrugs have a stronger ability to cross the gastrointestinal barrier. The results showed that the intestinal permeability of CTX increased after structural modification, which improved the oral absorption of CTX.

Subsequently, the effect of P-gp efflux on prodrug permeability was investigated. After adding the P-gp inhibitors, there was no significant difference in the uptake of CTX and the three prodrugs (Fig. 4G). On balance, prodrugs have poor affinity for P-gp efflux, which could greatly improve their oral absorption.

3.5. *In vitro reduction release of prodrugs*

Due to the specific metabolism of tumor cells, GSH levels are significantly higher in tumor cells than in normal cells [52,53]. Therefore, the effect of reduction-sensitive response modules with different steric hindrances on the activation of TG-like prodrugs was assessed *in vitro* to ensure that the parent drug was specifically released into tumor cells. As shown in Fig. 5A, CTX-S-S-TG was converted more quickly to CTX than CTX-(C)S-(C)S-TG at various concentrations of DTT. For instance, 55% of the CTX was released from CTX-S-S-TG at 48 h in the presence of 10 mM DTT, whereas 20% was released from the CTX-(C)S-(C)S-TG group under the same conditions. As the concentration of DTT was increased to 50 mM, more than 50% of the CTX was released from CTX-(C)S-(C)S-TG SNEDDS. In contrast, CTX-10C-TG showed no release of the parent drug in response to 10 or 50 mM DTT, which may be attributed to the lack of reduction-sensitive bonds in the structure of CTX-10C-TG. The above results indicate that CTX-(C)S-(C)S-TG could release active parent drugs specifically in highly reducing environments and might be more stable than CTX-S-S-TG in the presence of small amounts of reducing substances. The CTX release mechanisms of three TG-like prodrugs were summarized in Fig. 5B.

3.6. *Stability of the prodrugs in rat plasma*

Small amounts of reducing substances, such as GSH, exist in the blood circulation, which might pose challenges to prodrug stability [54]. The above reduction-release study preliminarily proved the reductive properties of CTX-S-S-TG and CTX-(C)S-(C)S-TG. Next, the stability of the three TG-like prodrugs in plasma supplemented with lipase or in a simulated tumor environment (high lipase activity and high DTT concentration) was investigated. As shown in Fig. 5C, the three prodrugs were first hydrolyzed into MG-like prodrugs by lipase. Furthermore, more than 65% of CTX-S-S-TG was converted to CTX after 8 h of incubation with plasma, owing to the influence of reducing substances (Fig. 5D). In contrast, only 35% of CTX was released from CTX-(C)S-(C)S-TG similar to the non-sensitive CTX-10C-TG. This chemical inertia could be attributed to the introduction of α- alkyl substitutions to the reduction-sensitive response module, elevating its stability. In the simulated tumor environment, the hydrolysis rate of the CTX-(C)S-(C)S-TG prodrug was accelerated, resulting in the rapid release of CTX, which may be attributed to the accelerated cleavage of disulfide bond in the presence of high concentrations of DTT (Fig. 5E and 5F). Due to the presence of a non-reduction-sensitive ester bond, the hydrolysis rate of CTX-10C-TG did not change significantly. The order of CTX release was as follows: CTX-S-S-TG > CTX-(C)S-(C)S-TG > CTX-10C-TG. Therefore, fine-tuning of the response module could influence the activation kinetics of prodrugs, which may further contribute to systemic toxicity and efficacy.

3.7. *In vitro cytotoxicity assay*

The cytotoxicity of the CTX solution and prodrug SNEDDS in tumor cells (RM-1 and MCF-7) and normal cells (3T3 cells) is displayed in Fig. 6A-6F. IC_{50} values of each group are shown in Fig. 6G-6H and Table S1. The CTX solution showed prominent dose-dependent cytotoxicity in both tumor and normal cells. The cytotoxicity of the three prodrug SNEDDS groups in RM-1 and MCF-7 cells was lower than that of the CTX solution group, which may be attributed to the delayed release of the active drug from the prodrug SNEDDS. Despite both CTX-S-S-TG and CTX-(C)S-(C)S-TG prodrug contained reduction-sensitive disulfide bonds, the cytotoxicity of CTX-(C)S-(C)S-TG prodrug group was slightly weaker than that of the CTX-S-S-TG prodrug group, due to the introduction of α-alkyl substitutions to the response module, influencing the chemical inertia. Nonetheless, the CTX-(C)S-(C)S-TG prodrug group showed stronger cytotoxicity than the CTX-10C-TG prodrug group in cancer cells, owing to the essential difference between reduction-sensitive and non-sensitive bonds. Unlike the CTX solution group, the CTX-S-S-TG, CTX-(C)S-(C)S-TG, and CTX-10C-TG prodrug groups exhibited low toxicity in 3T3 cells, highlighting the safety of the three prodrugs. Due to the existence of α- alkyl groups, CTX-(C)S-(C)S-TG was more stable than CTX-S-S-TG, which made CTX-(C)S-(C)S-TG less toxic to normal cells. CTX-10C-TG showed a toxicity similar to that of CTX-(C)S-(C)S-TG in normal cells, which could be attributed to the stability of non-sensitive bonds. The selectivity index (SI, IC_{50} of normal cell divided by IC_{50} of tumor cell) was used to evaluate the toxicity selectivity of the prodrugs and the parent drug for tumor cells and normal cells. A large SI value indicated that the drug had better safety and selectivity (Table 2). Owing to the high stability of the steric disulfide bond, the CTX-(C)S-(C)S-TG prodrug group exhibited higher SI values than the CTX-S-S-TG prodrug group. High-dose oral CTX may cause severe gastrointestinal toxicity; therefore, the toxicity of CTX prodrugs in Caco-2 cells was investigated. As shown in Fig. S13, the toxicity of the three CTX prodrug SNEDDS on Caco-2 cells was lower than that of CTX SNEDDS and CTX solution, proving the intestinal safety of the three prodrugs. The above results indicate that fine-tuning the response module can influence the efficacy and systemic security, which is expected to change the *in vivo* fate of chemotherapy drugs.

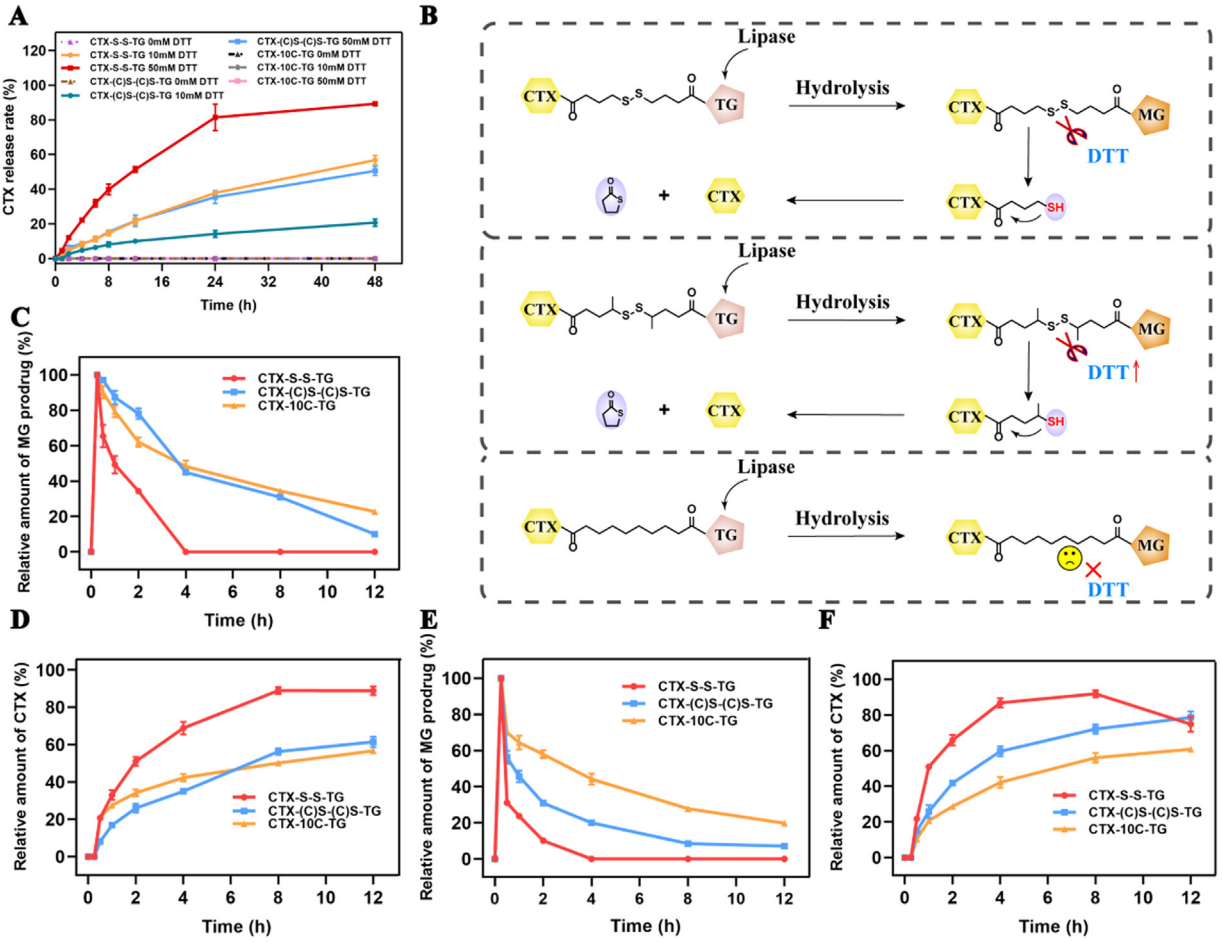

Fig. 5 – *In vitro* reduction-sensitive release and plasma stability of TG-like prodrugs. (A) CTX release from TG prodrugs with or without DTT. (B) The CTX release mechanisms of the three TG-like prodrugs. (C) Production of MG prodrugs or (D) CTX of all TG prodrugs in the plasma supplied with 1000 IU/ml lipase. (E) Production of MG prodrugs or (F) CTX of all TG prodrugs in the plasma supplied with 1000 IU/ml lipase and 50 mM DTT ($n = 3$).

Table 2 – Selectivity index (SI) of CTX and CTX TG-like prodrugs.

Formulations	RM-1		MCF-7	
	48 h	72 h	48 h	72 h
CTX solution	26.33	10.68	4.05	1.46
CTX-S-S-TG SNEDDS	42.46	30.40	24.74	19.11
CTX-(C)S-(C)S-TG SNEDDS	69.48	182.97	39.52	72.20
CTX-10C-TG SNEDDS	25.09	55.97	17.47	42.85

3.8. *In vivo oral pharmacokinetic study*

Subsequently, the *in vivo* pharmacokinetics of the CTX solution, CTX SNEDDS, and prodrug SNEDDS were investigated. The plasma concentration-time curves of free CTX are shown in Fig. 7A and 7B, and the pharmacokinetic parameters are shown in Table 3. The areas under the plasma concentration-time curves ($AUC_{0\text{-}24\ h}$) of CTX-S-S-TG SNEDDS, CTX-(C)S-(C)S-TG SNEDDS, and CTX-10C-TG SNEDDS were 19.1-, 11.5- and 5.4-fold greater than those of the CTX solution, respectively (Fig. 7C). In comparison with CTX solution (117.1 ± 48.5 ng/ml), C_{max} of CTX significantly increased with 546.0 ± 306.5 ng/ml of CTX-S-S-TG SNEDDS and 309.6 ± 22.2 ng/ml of CTX-(C)S-(C)S-TG SNEDDS. Correspondingly, the oral absolute bioavailabilities (F_{ab}) of the free parent drug released from two prodrugs were 59.2% and 35.6%, respectively, in stark contrast to that of the CTX solution (3.1%). The high F_{ab} indicated that the prodrug delivery strategy through lymphatic transport could improve oral absorption. However, CTX-S-S-TG group had a higher F_{ab} value than CTX-(C)S-(C)S-TG group, which might generate related systemic toxicity due to the premature

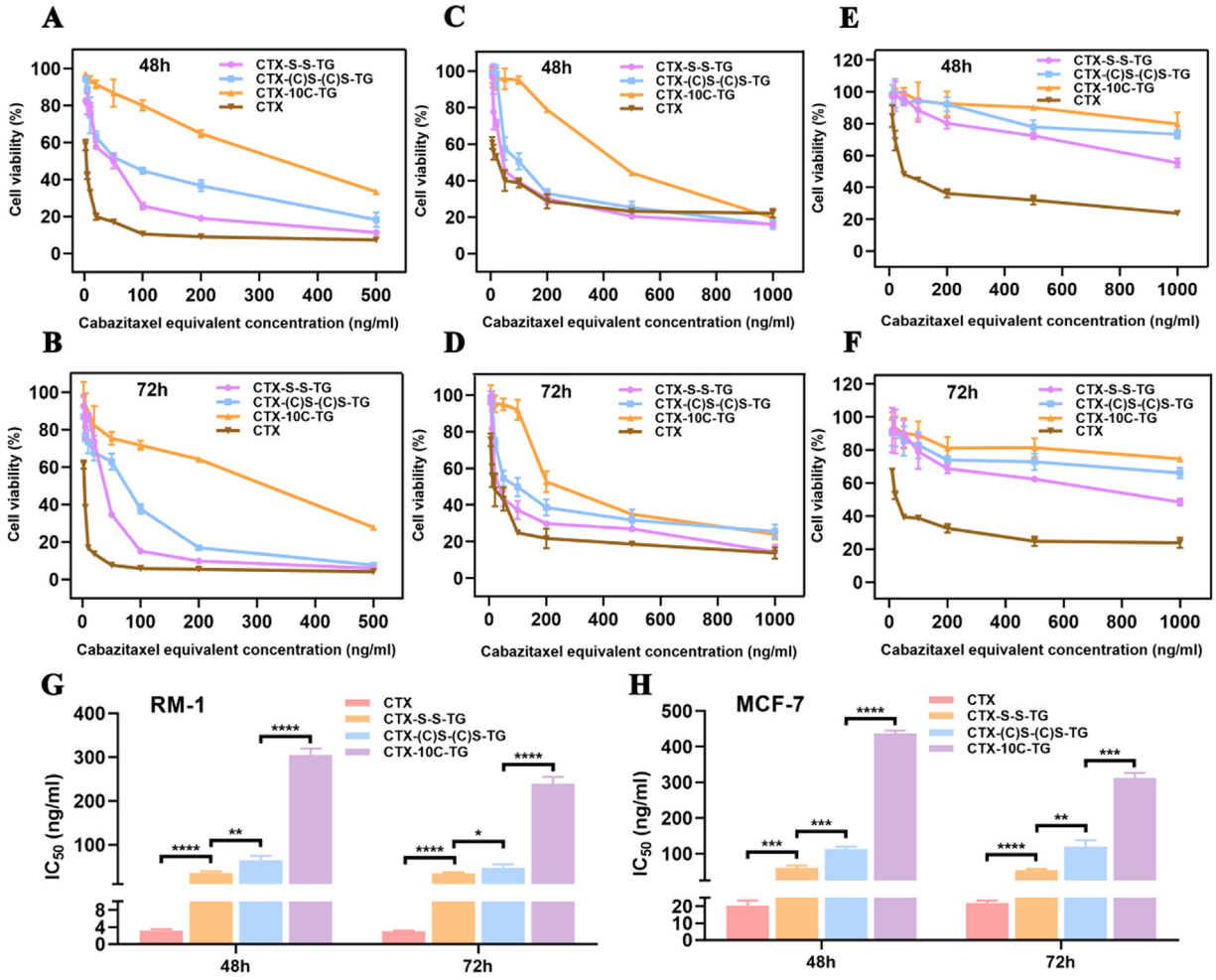

Fig. 6 – *In vitro* cytotoxicity of TG-like prodrugs. Cell viability of RM-1 cells after treatment with various concentrations of CTX solution, CTX-S-S-TG prodrug, CTX-(C)S-(C)S-TG prodrug and CTX-10C-TG prodrug SNEDDS for (A) 48 h and (B) 72 h. Cell viability of MCF-7 cells after treatment for (C) 48 h and (D) 72 h. Cell viability of 3T3 cells after treatment for (E) 48 h and (F) 72 h. IC_{50} of CTX solution and three CTX prodrug SNEDDS against tumor cells of (G) RM-1 cells and (H) MCF-7 cells at different time points. Data are presented as mean ± SD ($n = 3$); $^{**}P < 0.01$, $^{***}P < 0.001$, $^{****}P < 0.0001$.

Table 3 – Pharmacokinetic parameters of CTX solution, CTX SNEDDS, CTX-S-S-TG SNEDDS, CTX-(C)S-(C)S-TG SNEDDS and CTX-10C-TG SNEDDS after oral administration in rats (mean ± SD; $n = 3$).

Formulations	T_{max} (h)	C_{max} (ng/ml)	$T_{1/2}$ (h)	AUC_{0-}24 h (μg/l/h)	F_{rel}%	F_{ab}%
CTX Solution (i.v.)	0.083	5813.3 ± 92.9	2.3 ± 0.4	5061.6 ± 148.7	/	100
CTX Solution	0.3 ± 0.1	117.1 ± 48.5	12.7 ± 9.7	156.5 ± 39.0	100	3.1
CTX SNEDDS	0.8 ± 0.5	34.6 ± 4.9	9.4 ± 6.1	104.7 ± 4.0	66.9	2.1
CTX-S-S-TG SNEDDS	4	546.0 ± 306.5	1.5 ± 0.5	2996.4 ± 1100.2	1914.6	59.2
CTX-(C)S-(C)S-TG SNEDDS	4	309.6 ± 22.2	2.0 ± 0.6	1803.9 ± 123.5	1152.7	35.6
CTX-10C-TG SNEDDS	2.7 ± 1.2	155.6 ± 53.2	1.3 ± 0.1	849.1 ± 352.1	542.6	16.8

release of parent drugs. The plasma concentration of free CTX in the CTX-(C)S-(C)S-TG prodrug group was lower than that in the CTX-S-S-TG prodrug group, indicating that steric disulfide bonds improved the stability of the CTX-(C)S-(C)S-TG prodrug in blood circulation. These results were in good agreement with those of an *in vitro* plasma stability study.

After digestion, 2-MG prodrugs were absorbed into the intestinal cells and re-esterified with exogenous or endogenous long-chain fatty acids to generate a series of CTX TG prodrugs whose structures could not be determined, making it difficult to directly measure the total amount of the parent drug in the plasma. Thus, CTX-S-S-TG and CTX-(C)S-(C)S-TG were broken down by the disulfide bond-reducing

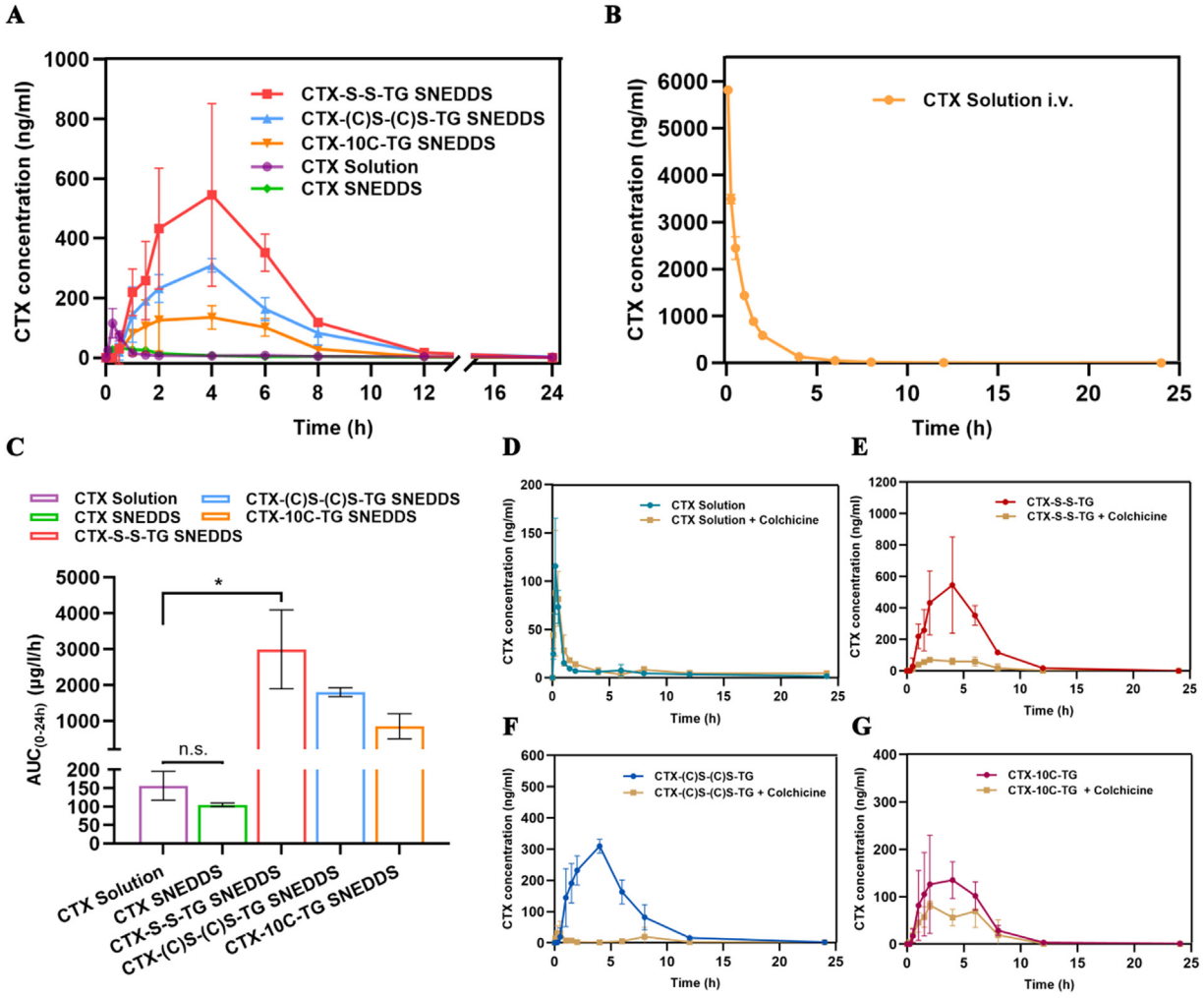

Fig. 7 – (A) Mean plasma concentration-time profiles of CTX solution, CTX SNEDDS, CTX-S-S-TG SNEDDS, CTX-(C)S-(C)S-TG SNEDDS and CTX-10C-TG SNEDDS after oral administration in rats. (B) Mean plasma concentration–time profiles of CTX solution after intravenous injection in rats. (C) The plasma AUC values of each oral group. (D-G) Mean plasma concentration–time profiles of CTX solution, CTX-S-S-TG SNEDDS, CTX-(C)S-(C)S-TG SNEDDS and CTX-10C-TG SNEDDS after oral administration to nontreated rats and to colchicine-treated rats 1 h before administration. Data are presented as mean ± SD ($n = 3$); *$P < 0.05$.

agent to release CTX. As shown in Fig. S14, the C_{max} of total CTX in CTX-S-S-TG and CTX-(C)S-(C)S-TG prodrugs was 4.4- and 5.7-fold higher, respectively, than that of free CTX. These results indicated that the majority of CTX was mainly present in the form of prodrugs in the blood circulation, and only small amounts of prodrugs were reduced by the reducing substance in the plasma, which also verified the good plasma stability of the prodrugs.

Natural long-chain TGs are normally absorbed into the blood circulation by the lymphatic system. To verify that the TG-like prodrugs could mimic the absorption pathway of natural TG, colchicine (5 mg/kg), an inhibitor of lymphatic transport, was used to inhibit the secretion of chylomicrons from enterocytes [55,56]. After the intraperitoneal injection of colchicine, the CTX plasma concentrations after oral administration of the three TG-like prodrug SNEDDS decreased significantly, while those after oral administration of the CTX solution were not affected (Fig. 7D-7G). The results showed that the TG module could endow prodrugs with the ability to assemble into LPs similar to natural TG and direct them into the mesenteric lymphatic system, bypassing first-pass metabolism.

3.9. *In vivo anti-tumor effect*

The *in vivo* anti-tumor efficiency of the TG-like prodrugs with different response modules was evaluated using a subcutaneous RM-1 xenograft model. As shown in Fig. 8B and 8E, there was no significant anti-tumor activity after the oral administration of the CTX solution and CTX SNEDDS. In contrast, CTX-S-S-TG and CTX-(C)S-(C)S-TG exhibited surprising tumor-suppressive effects owing to an increase in oral bioavailability and the introduction of reduction-sensitive bonds. However, the body weight of CTX-S-S-TG SNEDDS-

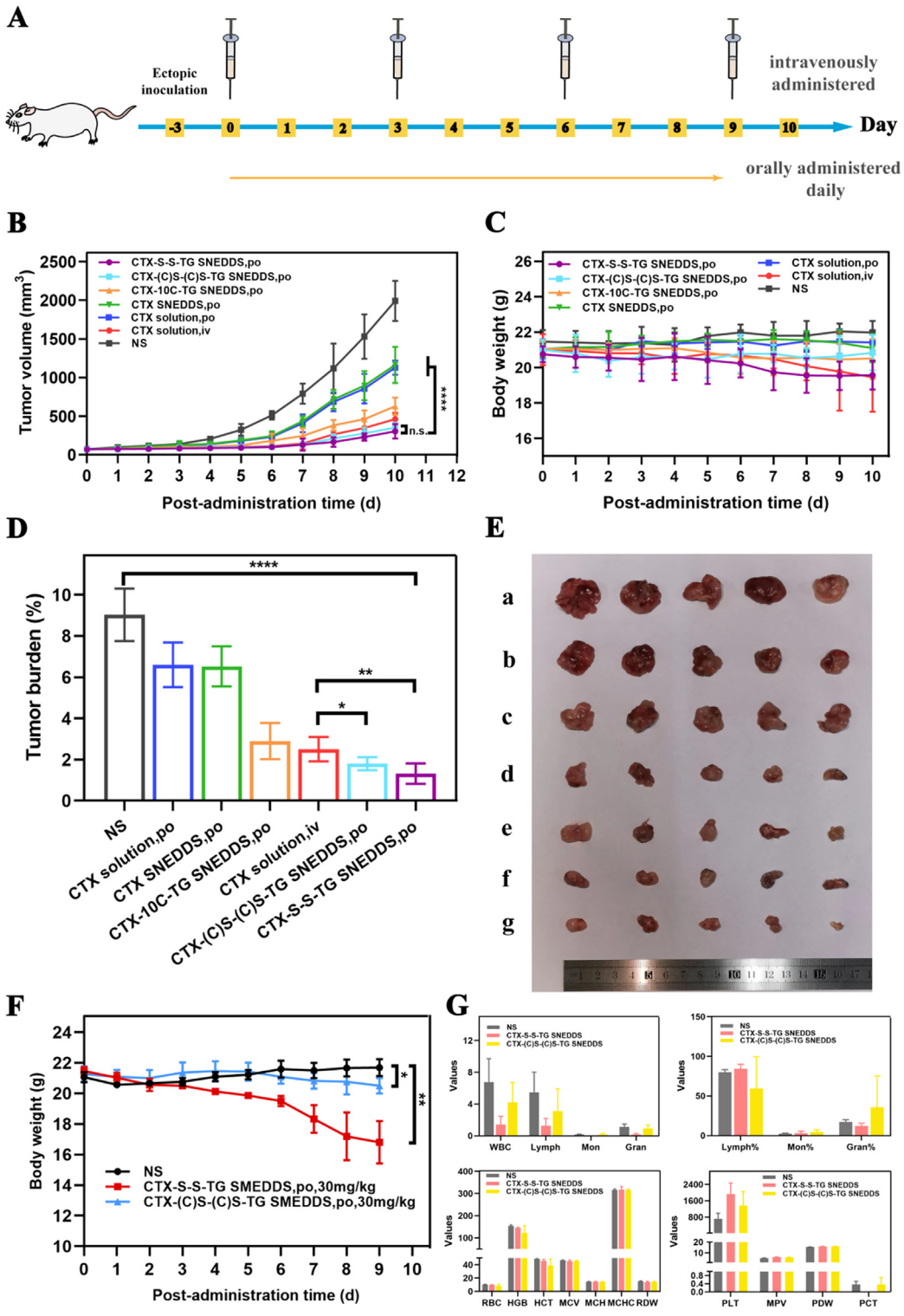

Fig. 8 – *In vivo* anti-tumor activity of prodrug against RM-1 xenograft tumors. (A) Schematic diagram of *in vivo* anti-tumor therapy. (B) Tumor volume-time curve, (C) body weight change and (D) tumor burden efficiency of each group. (E) Images of tumors after the last treatment: (a) NS, (b) CTX SNEDDS (p.o.), (c) CTX solution (p.o.), (d) CTX-10C-TG prodrug SNEDDS (p.o.), (e) CTX solution (i.v.), (f) CTX-(C)S-(C)S-TG prodrug SNEDDS (p.o.), and (g) CTX-S-S-TG prodrug SNEDDS (p.o.). (F) Body weight changes after oral administration of large doses of prodrugs. (G) Blood routine examination for C57BL/6 mice bearing RM-1 xenografts after oral administration of large doses of prodrugs. *$P < 0.05$, **$P < 0.01$, ****$P < 0.0001$, and n.s. = not significant ($n = 5$); determined by two-tailed Student's t-test.

treated mice showed a downward trend, which might be attributed to the early leakage of the active parent drug into the blood circulation (Fig. 8C). In comparison, there were no significant changes in body weight between the CTX-(C)S-(C)S-TG and CTX-10C-TG SNEDDS groups. Consistent with Wang's research, disulfide bonds with steric protection are less sensitive to the reduction environment *in vivo*, which is actually beneficial to avoid premature drug release [57]. Our research also verified that steric disulfide bonds could be applied to oral delivery of small molecular drugs, which avoid the premature drug release. As shown in Fig. 8D, CTX-S-S-TG and CTX-(C)S-(C)S-TG had comparable tumor burdens, which also demonstrated the good anti-tumor effect of the disulfide bond-bridged prodrugs. The non-sensitive CTX-10C-TG prodrug group was difficult to release active drug, which led to a larger tumor volume and higher tumor-bearing rate than the disulfide bond-based prodrug groups.

The systemic safety and gastrointestinal toxicity of TG-like prodrugs (p.o.) and CTX solution (i.v.) were evaluated. H&E-stained pathological examinations of major organs (heart, liver, spleen, lung, and kidney) and gastrointestinal tissues (stomach, duodenum, jejunum, ileum and colon) are shown in Figs. S15 and S16, respectively. There was no obvious histological damage in the H&E-stained sections of the major organs or gastrointestinal tissue in the CTX-(C)S-(C)S-TG SNEDDS group. Additionally, hepatorenal function parameters and blood routine examinations were performed after the last day (Figs. S17 and S18). The AST and ALT levels in the intravenous CTX solution group were abnormal, indicating potential hepatotoxicity. Decreased numbers of leukocytes and neutrophils also indicated bone marrow hematopoiesis suppression caused by the intravenous CTX solution. In contrast, there were no differences in routine blood test results between the CTX-(C)S-(C)S-TG SNEDDS and normal saline (NS) groups.

As the mice were administered high doses of CTX-S-S-TG and CTX-(C)S-(C)S-TG orally, the body weight of the CTX-S-S-TG SNEDDS group showed a significant downward trend, whereas that of the CTX-(C)S-(C)S-TG group was not significantly different from that of the NS group (Fig. 8F). Furthermore, there were no obvious abnormalities in the blood routine consequence of the CTX-(C)S-(C)S-TG SNEDDS group (Fig. 8G). These results demonstrate that CTX-(C)S-(C)S-TG SNEDDS can effectively inhibit tumor growth and greatly reduce the systemic and gastrointestinal toxicity of CTX after fine-tuning the reduction-sensitive response module.

4. Conclusion

In summary, a series of TG-like prodrugs with different response modules that could mimic the lymphatic transport mechanism of natural TGs were synthesized. Compared to the CTX parent drug, TG-like prodrugs exhibit excellent digestibility and intestinal penetration owing to the presence of an intestinal lymph vessel-directed triglyceride module, favoring the oral bioavailability of CTX. Constructional differences in the response modules endowed the three prodrugs with diverse features. The CTX-S-S-TG prodrug possessed the highest release rate of the active drug and the best anti-tumor activity, owing to its reduction-sensitive disulfide bond. Nevertheless, the oversensitive response module caused the CTX-S-S-TG prodrug to crack ahead of time in the blood circulation, resulting in severe systemic toxicity. The CTX-10C-TG prodrug was more stable in blood circulation, but non-reduction-sensitive response module prevented CTX-10C-TG from releasing CTX successfully. Benefitting from the fine-tuning of the disulfide bond-containing response module, CTX-(C)S-(C)S-TG exhibited a plasma stability similar to that of CTX-10C-TG and acceptable reduction sensitivity. To sum up, CTX-(C)S-(C)S-TG has excellent gastric stability and intestinal permeability, which is conducive to improving the oral bioavailability and the efficiency of reaching the target site. Excellent lymphatic transport ability enables CTX-(C)S-(C)S-TG prodrug to bypass the hepatic first-pass effect and improve the oral bioavailability. Modest reduction sensitivity and acceptable plasma stability guarantee the anti-tumor efficacy and safety of prodrugs. Thus, the fine-tuning of the reduction-sensitive response module of the TG-like prodrug is expected to improve the oral bioavailability and systemic safety of oral prodrugs while maintaining excellent anti-tumor efficacy. Our research on different response modules on TG-like prodrugs opened new therapeutic horizons to design safe and effective prodrugs. More drugs with low oral absorption and high toxicity can benefit from the strategy of fine-tuning activation behaviors for future studies.

Conflicts of interest

The authors declare that they have no known competing financial interests or personal relationships that could have appeared to influence the work reported in this paper.

Acknowledgments

This work was financially supported by National Natural Science Foundation of China (No. 82173766, 82104109), Natural Science Foundation of Liaoning Province (2022-BS-158), Liaoning Province Applied Basic Research Program (No. 2022JH2/101300097) and National Key R&D Program of China (No. 2022YFE0111600).

Supplementary materials

Supplementary material associated with this article can be found, in the online version, at doi:10.1016/j.ajps.2024.100908.

References

[1] Moore S. Facilitating oral chemotherapy treatment and compliance through patient/family-focused education. Cancer Nurs 2007;30(2):112–22 quiz 123-4.
[2] Pobel C, Auclin E, Teyssonneau D, Laguerre B, Cancel M, Boughalem E, et al. Cabazitaxel multiple rechallenges in metastatic castration-resistant prostate cancer. Cancer Med 2021;10(18):6304–9.

[3] Sun B, Lovell JF, Zhang Y. Current development of cabazitaxel drug delivery systems. Wiley Interdiscip Rev Nanomed Nanobiotechnol 2023;15(2):e1854.
[4] Sun Y, Lee RJ, Meng F, Wang G, Zheng X, Dong S, et al. Microfluidic self-assembly of high cabazitaxel loading albumin nanoparticles. Nanoscale 2020;12(32):16928–16933.
[5] Chen Y, Pan Y, Hu D, Peng J, Hao Y, Pan M, et al. Recent progress in nanoformulations of cabazitaxel. Biomed Mater 2021;16(3):2002.
[6] Heidenreich A, Scholz HJ, Rogenhofer S, Arsov C, Retz M, Müller SC, et al. Cabazitaxel plus prednisone for metastatic castration-resistant prostate cancer progressing after docetaxel: results from the German compassionate-use programme. Eur Urol 2013;63(6):977–82.
[7] Fumoleau P, Trigo JM, Isambert N, Sémiond D, Gupta S, Campone M. Phase I dose-finding study of cabazitaxel administered weekly in patients with advanced solid tumours. BMC Cancer 2013;13:460.
[8] Franco V, Gershkovich P, Perucca E, Bialer M. The interplay between liver first-pass effect and lymphatic absorption of cannabidiol and its implications for cannabidiol oral formulations. Clin Pharmacokinet 2020;59(12):1493–1500.
[9] Sun M, Zhai X, Xue K, Hu L, Yang X, Li G, et al. Intestinal absorption and intestinal lymphatic transport of sirolimus from self-microemulsifying drug delivery systems assessed using the single-pass intestinal perfusion (SPIP) technique and a chylomicron flow blocking approach: linear correlation with oral bioavailabilities in rats. Eur J Pharm Sci 2011;43(3):132–40.
[10] Xu Q, Zhou A, Wu H, Bi Y. Development and *in vivo* evaluation of baicalin-loaded W/O nanoemulsion for lymphatic absorption. Pharm Dev Technol 2019;24(9):1155–63.
[11] Kim KS, Suzuki K, Cho H, Youn YS, Bae YH. Oral nanoparticles exhibit specific high-efficiency intestinal uptake and lymphatic transport. ACS Nano 2018;12(9):8893–900.
[12] Liu R, Luo C, Pang Z, Zhang J, Ruan S, Gao H, et al. Advances of nanoparticles as drug delivery systems for disease diagnosis and treatment. Chin Chem Lett 2023;34(2):107518.
[13] Dahan A, Zimmermann EM, Ben-Shabat S. Modern prodrug design for targeted oral drug delivery. Molecules 2014;19(10):16489–505.
[14] Vohidov F, Andersen JN, Economides KD, Shipitsin MV, Burenkova O, Ackley JC, et al. Design of BET inhibitor bottlebrush prodrugs with superior efficacy and devoid of systemic toxicities. J Am Chem Soc 2021;143(12):4714–24.
[15] Rautio J, Kumpulainen H, Heimbach T, Oliyai R, Oh D, Järvinen T, et al. Prodrugs: design and clinical applications. Nat Rev Drug Discov 2008;7(3):255–70.
[16] Lambert DM. Rationale and applications of lipids as prodrug carriers. Eur J Pharm Sci 2000;11(2):S15–27 Suppl.
[17] Markovic M, Ben-Shabat S, Keinan S, Aponick A, Zimmermann EM, Dahan A. Lipidic prodrug approach for improved oral drug delivery and therapy. Med Res Rev 2019;39(2):579–607.
[18] Dahan A, Duvdevani R, Shapiro I, Elmann A, Finkelstein E, Hoffman A. The oral absorption of phospholipid prodrugs: *in vivo* and *in vitro* mechanistic investigation of trafficking of a lecithin-valproic acid conjugate following oral administration. J Control Release 2008;126(1):1–9.
[19] Wang H, Feng Z, Wu D, Fritzsching KJ, Rigney M, Zhou J, et al. Enzyme-regulated supramolecular assemblies of cholesterol conjugates against drug-resistant ovarian cancer cells. J Am Chem Soc 2016;138(34):10758–61.
[20] Bala V, Rao S, Li P, Wang S, Prestidge CA. Lipophilic prodrugs of SN38: synthesis and *in vitro* characterization toward oral chemotherapy. Mol Pharm 2016;13(1):287–94.
[21] Sun Y, Zhao D, Wang G, Jiang Q, Guo M, Kan Q, et al. A novel oral prodrug-targeting transporter MCT 1: 5-fluorouracil-dicarboxylate monoester conjugates. Asian J Pharm Sci 2019;14(6):631–9.
[22] Skakkebaek NE, Bancroft J, Davidson DW, Warner P. Androgen replacement with oral testosterone undecanoate in hypogonadal men: a double blind controlled study. Clin Endocrinol 1981;14(1):49–61.
[23] Ravotti R, Worlitschek J, Pulham CR, Stamatiou A. Triglycerides as novel phase-change materials: a review and assessment of their thermal properties. Molecules 2020;25(23):5572.
[24] Nancy BK, Evelien R, Portia SL, Alison JF, Brea CL, Wendy AW, et al. Lipoprotein lipase links dietary fat to solid tumor cell proliferation. Mol Cancer Ther 2011;10(3):427–36.
[25] Wang X, Zhang C, Han N, Luo J, Zhang S, Wang C, et al. Triglyceride-mimetic prodrugs of scutellarin enhance oral bioavailability by promoting intestinal lymphatic transport and avoiding first-pass metabolism. Drug Deliv 2021;28(1):1664–72.
[26] Debajyoti G. Lipase catalysis in mixed micelles. ChemBioEng Rev 2022;9(4):409–18.
[27] Mu H, Høy CE. The digestion of dietary triacylglycerols. Prog Lipid Res 2004;43(2):105–33.
[28] Gracia G, Cao E, Feeney OM, Johnston APR, Porter CJH, Trevaskis NL. High-density lipoprotein composition influences lymphatic transport after subcutaneous administration. Mol Pharm 2020;17(8):2938–51.
[29] Hu L, Quach T, Han S, Lim SF, Yadav P, Senyschyn D, et al. Glyceride-mimetic prodrugs incorporating self-immolative spacers promote lymphatic transport, avoid first-pass metabolism, and enhance oral bioavailability. Angew Chem Int Ed Engl 2016;55(44):13700–5.
[30] Han S, Quach T, Hu L, Wahab A, Charman WN, Stella VJ, et al. Targeted delivery of a model immunomodulator to the lymphatic system: comparison of alkyl ester *versus* triglyceride mimetic lipid prodrug strategies. J Control Release 2014;177:1–10.
[31] Miao Y, Ye Q, Zhang M, Gao L, Wang X, Zhong W, et al. Enhancing oral performance of paclitaxel lipid-mimic prodrug via modulating type of fatty acids. Adv Healthc Mater 2023;12(19):e2203118.
[32] Wang H, Lu Q, Miao Y, Song J, Zhang M, Wang Z, et al. Boosting SN38-based oral chemotherapy to combine reduction-bioactivated structured lipid-mimetic prodrug with ascorbic acid. Nano Res 2022;15(10):9092–104.
[33] Dagogo-Jack I, Shaw AT. Tumour heterogeneity and resistance to cancer therapies. Nat Rev Clin Oncol 2018;15(2):81–94.
[34] Hida K, Maishi N, Sakurai Y, Hida Y, Harashima H. Heterogeneity of tumor endothelial cells and drug delivery. Adv Drug Deliv Rev 2016;99(Pt B):140–7.
[35] Wang D, Li L, Xu H, Sun Y, Li W, Liu T, et al. Rational engineering docetaxel prodrug nanoassemblies: response modules guiding efficacy enhancement and toxicity reduction. Nano Lett 2023;23(8):3549–57.
[36] Ye J, Hou B, Chen F, Zhang S, Xiong M, Li T, et al. Bispecific prodrug nanoparticles circumventing multiple immune resistance mechanisms for promoting cancer immunotherapy. Acta Pharm Sin B 2022;12(6):2695–709.
[37] Jeong GW, Jeong YI, Nah JW. Triggered doxorubicin release using redox-sensitive hyaluronic acid-g-stearic acid micelles for targeted cancer therapy. Carbohydr Polym 2019;209:161–71.
[38] Tian C, Guo J, Wang G, Sun B, Na K, Zhang X, et al. Efficient intestinal digestion and on site tumor-bioactivation are the two important determinants for chylomicron-mediated lymph-targeting triglyceride-mimetic docetaxel oral prodrugs. Adv Sci 2019;6(24):1901810.

[39] Climent MÁ, Pérez-Valderrama B, Mellado B, Fernández Parra EM, Fernández Calvo O, Ochoa de Olza M, et al. Weekly cabazitaxel plus prednisone is effective and less toxic for 'unfit' metastatic castration-resistant prostate cancer: phase II Spanish Oncology Genitourinary Group (SOGUG) trial. Eur J Cancer 2017;87:30–7.
[40] Zhang J, Zhang Y, Huang Y, Wang D, Zuo S, Xu H. Rational design of tumor-selective prodrug nanoassemblies: greatly improving the *in vivo* fate and tolerability of high-toxic cabazitaxel. Chem Eng J 2023;458:141510.
[41] Shi L, Wang Y, Wang Q, Jiang Z, Ren L, Yan Y, et al. Transforming a toxic drug into an efficacious nanomedicine using a lipoprodrug strategy for the treatment of patient-derived melanoma xenografts. J Control Release 2020;324:289–302.
[42] Su D, Zhang D. Linker design impacts antibody-drug conjugate pharmacokinetics and efficacy via modulating the stability and payload release efficiency. Front Pharmacol 2021;12:687926.
[43] Erickson HK, Widdison WC, Mayo MF, Whiteman K, Audette C, Wilhelm SD, et al. Tumor delivery and *in vivo* processing of disulfide-linked and thioether-linked antibody-maytansinoid conjugates. Bioconjug Chem 2010;21(1):84–92.
[44] Kellogg BA, Garrett L, Kovtun Y, Lai KC, Leece B, Miller M, et al. Disulfide-linked antibody-maytansinoid conjugates: optimization of *in vivo* activity by varying the steric hindrance at carbon atoms adjacent to the disulfide linkage. Bioconjug Chem 2011;22(4):717–27.
[45] Cui W, Zhang S, Zhao H, Luo C, Sun B, Li Z, et al. Formulating a single thioether-bridged oleate prodrug into a self-nanoemulsifying drug delivery system to facilitate oral absorption of docetaxel. Biomater Sci 2019;7(3):1117–31.
[46] Wang Y, Luo C, Zhou S, Wang X, Zhang X, Li S, et al. Investigating the crucial roles of aliphatic tails in disulfide bond-linked docetaxel prodrug nanoassemblies. Asian J Pharm Sci 2021;16(5):643–52.
[47] Li L, Zuo S, Dong F, Liu T, Gao Y, Yang Y, et al. Small changes in the length of diselenide bond-containing linkages exert great influences on the antitumor activity of docetaxel homodimeric prodrug nanoassemblies. Asian J Pharm Sci 2021;16(3):337–49.
[48] Sek L, Porter CJ, Charman WN. Characterisation and quantification of medium chain and long chain triglycerides and their *in vitro* digestion products, by HPTLC coupled with *in situ* densitometric analysis. J Pharm Biomed Anal 2001;25(3–4):651–61.
[49] Hidalgo IJ, Raub TJ, Borchardt RT. Characterization of the human colon carcinoma cell line (Caco-2) as a model system for intestinal epithelial permeability. Gastroenterology 1989;96(3):736–49.
[50] Kim HJ, Huh D, Hamilton G, Ingber DE. Human gut-on-a-chip inhabited by microbial flora that experiences intestinal peristalsis-like motions and flow. Lab Chip 2012;12(12):2165–74.
[51] Artursson P, Palm K, Luthman K. Caco-2 monolayers in experimental and theoretical predictions of drug transport. Adv Drug Deliv Rev 2001;46(1–3):27–43.
[52] Wang Z, Xu K, Wang G, Durrani S, Lin F, Wu F. One stone, five birds": ultrabright and multifaceted carbon dots for precise cell imaging and glutathione detection. Chem Eng J 2023;457:140997.
[53] Li X, Wang H, Zhang Y, Cao Q, Chen Y. A GSH-responsive PET-based fluorescent probe for cancer cells imaging. Chin Chem Lett 2021;32:1541–4.
[54] Mo R, Gu Z. Tumor microenvironment and intracellular signal-activated nanomaterials for anticancer drug delivery. Mater Today 2016;19:274–83.
[55] Glickman RM, Perrotto JL, Kirsch K. Intestinal lipoprotein formation: effect of cholchicine. Gastroenterology 1976;70(3):347–52.
[56] Arreaza-Plaza CA, Bosch V, Otayek MA. Lipid transport across the intestinal epithelial cell. Effect of colchicine. Biochim Biophys Acta 1976;431(2):297–302.
[57] Wang Q, Guan J, Wan J, Li Z. Disulfide based prodrugs for cancer therapy. RSC Adv 2020;10(41):24397–409.